Stable ATP binding mediated by a partial NBD dimer of the CFTR chloride channel

Ming-Feng Tsai,[1,2] Min Li,[2] and Tzyh-Chang Hwang[1,2]

[1]Department of Medical Pharmacology and Physiology and [2]Dalton Cardiovascular Research Center, University of Missouri, Columbia, MO 65211

Cystic fibrosis transmembrane conductance regulator (CFTR), a member of the adenosine triphosphate (ATP) binding cassette (ABC) superfamily, is an ATP-gated chloride channel. Like other ABC proteins, CFTR encompasses two nucleotide binding domains (NBDs), NBD1 and NBD2, each accommodating an ATP binding site. It is generally accepted that CFTR's opening–closing cycles, each completed within 1 s, are driven by rapid ATP binding and hydrolysis events in NBD2. Here, by recording CFTR currents in real time with a ligand exchange protocol, we demonstrated that during many of these gating cycles, NBD1 is constantly occupied by a stably bound ATP or 8-N_3-ATP molecule for tens of seconds. We provided evidence that this tightly bound ATP or 8-N_3-ATP also interacts with residues in the signature sequence of NBD2, a telltale sign for an event occurring at the NBD1–NBD2 interface. The open state of CFTR has been shown to represent a two-ATP–bound NBD dimer. Our results indicate that upon ATP hydrolysis in NBD2, the channel closes into a "partial NBD dimer" state where the NBD interface remains partially closed, preventing ATP dissociation from NBD1 but allowing the release of hydrolytic products and binding of the next ATP to occur in NBD2. Opening and closing of CFTR can then be coupled to the formation and "partial" separation of the NBD dimer. The tightly bound ATP molecule in NBD1 can occasionally dissociate from the partial dimer state, resulting in a nucleotide-free monomeric state of NBDs. Our data, together with other structural/functional studies of CFTR's NBDs, suggest that this process is poorly reversible, implying that the channel in the partial dimer state or monomeric state enters the open state through different pathways. We therefore proposed a gating model for CFTR with two distinct cycles. The structural and functional significance of our results to other ABC proteins is discussed.

The Journal of General Physiology

INTRODUCTION

The CFTR, whose dysfunction results in the lethal genetic disease cystic fibrosis, is a unique member in the ATP binding cassette (ABC) transporter superfamiliy (Riordan et al., 1989), in that it functions as a chloride ion channel (Bear et al., 1992). ABC proteins possess two nucleotide binding domains (NBDs), NBD1 and NBD2, and two transmembrane domains (TMDs). The TMDs are structurally diversified to fulfill their distinct roles in accommodating different substrates for transport. However, NBDs, the energy–harvest machine, are highly conserved among members in this family. All NBDs share the same basic architecture (for review see Davidson and Chen, 2004; Oswald et al., 2006), with a larger core subdomain (head) comprising an ATP binding site that binds and hydrolyzes ATP and a smaller helical subdomain (tail) containing the ABC signature sequence (LSGGQ), so called because it is the hallmark of ABC proteins. High resolution crystal structures (for example, Smith et al., 2002; Chen et al., 2003; Zaitseva et al., 2005) have demonstrated that NBD1 and NBD2 rest monomerically without nucleotide, whereas in the presence of ATP, they coalesce into a head-to-tail dimer with two ATPs buried at interfacial ATP binding pockets, where each ATP bound in the head subdomain of one NBD also interacts with the tail subdomain of the partner NBD.

CFTR can be classified into a group of "asymmetric" ABC proteins, which typically exist in eukaryotes and, less frequently, in bacteria (for review see Procko et al., 2009). This asymmetry is so defined because of the finding that in some ATP-interacting motifs, including those critical for catalyzing ATP hydrolysis, CFTR's NBD2 retains all conserved residues, but its NBD1 presents several nonconsensus substitutions. An expected functional consequence of this structural asymmetry is that the NBD1 of CFTR displays a much lower catalytic ability than NBD2. This prediction appears to be supported by two lines of experimental approaches. First, photolabeling experiments demonstrated that 8-N_3ATP is occluded in NBD1 for tens of minutes, even with extensive washing, but is turned over quickly in NBD2

Correspondence to Tzyh-Chang Hwang: hwangt@health.missouri.edu

Abbreviations used in this paper: ABC, ATP binding cassette; CHO, Chinese hamster ovary; NBD, nucleotide binding domain; PATP, N^6-(2-phenylethyl)-ATP; PPi, pyrophosphate; TMD, transmembrane domain; WT, wild-type.

The Rockefeller University Press $30.00
J. Gen. Physiol. Vol. 135 No. 5 399–414
www.jgp.org/cgi/doi/10.1085/jgp.201010399

(Aleksandrov et al., 2002; Basso et al., 2003). Second, our previous study (Tsai et al., 2009) using electrophysiological recordings has shown that rapid ATP hydrolysis in NBD2 closes wild-type (WT) CFTR into an intermediate state with a lifetime of many seconds, during which an ATP molecule remains bound in NBD1. This single-ATP–bound intermediate state is distinguishable from the nucleotide-free state because of its exceptionally robust response to pyrophosphate (PPi).

A careful examination of these biochemical and functional results, however, reveals several potential problems. It can be seen from monomeric structures of CFTR's NBD1 (Lewis et al., 2004, 2005) that the ATP binding site is well exposed to the aqueous environment. Therefore, even though NBD1 may have reduced ATPase activity, it seems inconceivable that ATP can stay bound for seconds (Tsai et al., 2009) or even minutes (Basso et al., 2003). This puzzle might be explained by a simple hypothesis that the stably bound ATP molecule is "trapped" by the NBD1 head and the NBD2 tail at the dimer interface. Nonetheless, it was reported that a mutant CFTR with the whole NBD2 truncated (ΔNBD2-CFTR) still occludes 8-N_3ATP for minutes (Aleksandrov et al., 2008). Moreover, phosphorylation of CFTR, known to facilitate cross-linking of CFTR's two NBDs into a head-to-tail dimer configuration (Mense et al., 2006) and play a critical role in the opening of the CFTR channel through ATP-dependent dimerization of NBDs (for review see Gadsby et al., 2006; Chen and Hwang 2008), bears little influence on the occlusion of 8-N_3ATP by WT-CFTR (Basso et al., 2003).

Although the aforementioned photolabeling experiments provide results that contradict the idea of a dimer-mediated ATP trapping, our functional studies (Tsai et al., 2009) implicate a role played by both the head of NBD1 and the tail of NBD2 in regulating the stability of the single-ATP–bound state. Regardless of this mechanistic difference, it is also unclear why the ATP dwell times in NBD1 measured by these two sets of approaches differ by >50-fold. These conflicting ideas as well as results prompt us to design a real-time ligand exchange experiment to further investigate the structural and kinetic mechanisms by which stable ATP binding in NBD1 is attained. Our results suggest that a tight binding of ATP and 8-N_3ATP in the head of NBD1 requires interactions of the nucleotide with the tail of NBD2.

These findings lead to the establishment of a molecular model, where the dominant opening–closing cycle of CFTR is coupled to the interconversion of NBDs between a full dimer state and a "partial dimer" state, where the two NBDs are partially connected by the stably bound ATP molecule in NBD1, allowing nucleotide exchange to occur only in NBD2. Based on further experimental results, we were able to demonstrate a second gating cycle of CFTR involving a rare, complete disengagement of the two NBDs. The structural/functional implications of this new molecular model for other ABC proteins will be discussed.

MATERIALS AND METHODS

Cell culture and transient expression system

All membrane patches used in this study were from Chinese hamster ovary (CHO) cells, which were grown at 37°C in Dulbecco's Modified Eagle's Medium supplemented with 10% fetal bovine serum. The cDNA constructs of CFTR were cotransfected with pEGFP-C3 (Takara Bio Inc.), encoding the green fluorescence protein, using transfection reagent (PolyFect; QIAGEN). The transfected CHO cells were plated on sterile glass chips in 35-mm tissue dishes. Electrophysiological experiments were performed 2–4 d after transfection.

Electrophysiological recordings

Patch clamp pipettes were prepared from borosilicate capillary glass using a Flaming/Brown-type micropipette puller (P97; Sutter Instrument Co.). The pipette tips were then fire-polished with a homemade microforge to ∼1 μm external diameter, resulting in a pipette resistance of 2 to ∼4 MΩ in the bath solution in a continuously perfused recording chamber located on the stage of an inverted microscope (Olympus). Glass chips containing transfected CHO cells were transferred to the chamber before recordings. After inside-out patches with a seal resistance of >40 GΩ were obtained, CFTR channel currents were recorded at room temperature with an EPC-10 patch clamp amplifier (HEKA), filtered at 100 Hz with an eight-pole Bessel filter (Warner Instruments), and captured onto a hard disk at a sampling frequency of 500 Hz. The membrane potential was held at −60 mV, and the inward current in all figures was inverted for clearer data presentation.

All experiments were performed with a fast solution exchange device (SF-77B; Warner Instruments). To test the dead time of our solution exchange, we perfused two solutions with different concentrations of NaCl to the patch pipette. The exponential fit of the resulting current changes yielded a dead time of ∼30 ms (Tsai et al., 2009).

Chemicals and composition of solutions

The pipette solution contained (in mM): 140 NMDG chloride (NMDG-Cl), 2 $MgCl_2$, 5 $CaCl_2$, and 10 HEPES, pH 7.4 with NMDG. Cells were perfused with a bath solution containing (in mM): 145 NaCl, 5 KCl, 2 $MgCl_2$, 1 $CaCl_2$, 5 glucose, 5 HEPES, and 20 sucrose, pH 7.4 with NaOH. After the establishment of an inside-out configuration, the patch was perfused with a standard perfusion solution (i.e., intracellular solution) containing (in mM): 150 NMDG-Cl, 2 $MgCl_2$, 10 EGTA, and 8 Tris, pH 7.4 with NMDG.

MgATP and PKA were purchased from Sigma-Aldrich. 8-N_3-ATP was obtained from MP Biomedicals. N^6-(2-phenylethyl)-ATP (PATP) was from Biolog Life Science Institute. MgATP and 8-N_3-ATP were stored, respectively, in 250- and 10-mM stock solutions at −20°C. PATP stock solution was 10 mM and was stored at −60°C. All nucleotides were dissolved in perfusion solution for the experiments, and the pH was adjusted to 7.4 with NMDG.

Data analysis and statistics

Recordings from patches containing one CFTR channel were selected for single-channel kinetic analysis. These data were further filtered at 50 Hz and analyzed using software written by L. Csanády (Csanády, 2000). A three-state kinetic model, C↔O↔B, was adopted to extract ATP-dependent kinetic parameters as described previously (Bompadre et al., 2005). Macroscopic current recordings were

analyzed using the Igor Pro program (version 4.07; WaveMetrics). Current relaxations were fitted with single- or double-exponential function using a Levenberg-Marquardt–based algorithm within the Igor Pro program. All results are presented as means ± SEM; *n* represents the number of independent experiments. Student's *t* test was performed with Sigmaplot (version 8.0; SPSS Science). $P < 0.01$ was considered significant.

To convert the time constants presented in Fig. 10 E to the percentage of channels with ligand exchange that occurred in NBD1 (y axis of Fig. 10 F), we solved the following equations:

$$y + a = 100\%$$

$$72.4y + 30.5a = b,$$

where y is the percentage of CFTR with PATP bound in NBD1 (y value in Fig. 10 F); a is the percentage of CFTR with ATP bound in NBD1; 30.5 s is the current decay time constant measured when CFTR is only exposed to ATP plus PPi; 72.4 s is the current decay time constant measured when CFTR is only exposed to PATP plus PPi; and b is the current decay time constant measured when CFTR originally opened by ATP plus PPi was subsequently treated with different durations of PATP plus PPi (y value in Fig. 10 E).

Online supplemental material

Figs. S1 and S2 show raw traces of ligand exchange experiments conducted with mutations in NBD2's signature sequence. Figs. S3 and S4 present the biophysical properties of 8-N_3-ATP–gated WT-CFTR channels. Figs. S5 and S6 are control experiments for ATP/PATP exchange experiments with G551D-CFTR. Figs. S1–S6 are available at http://www.jgp.org/cgi/content/full/jgp.201010399/DC1.

RESULTS

Ligand exchange experiments reveal stable ATP binding in NBD1 during CFTR gating

As an opening–closing cycle of CFTR lasts for ~1 s (Zeltwanger et al., 1999; Vergani et al., 2003), biochemical demonstrations of the occlusion of 8-N_3ATP in NBD1 for tens of minutes described in the Introduction lead to the proposition that an ATP molecule can remain bound in CFTR's NBD1 for many gating cycles without dissociation (Basso et al., 2003; Gadsby et al., 2006). However, this contention needs more direct experimental evidence for the following reasons. First, tight ATP binding in NBD1 is so far only observed under conditions when CFTR is kept in a closed state in membrane patches (Tsai et al., 2009) or when CFTR proteins are in biochemical buffers, where their functional state is unknown (Aleksandrov et al., 2002; Basso et al., 2003). Thus, it has not been demonstrated directly that an ATP molecule stays tightly bound in NBD1 for repeated gating cycles. Second, even if those functional and biochemical data can be used to support this idea, the dramatic difference in the measured dwell time for the trapped ATP between these two assays would have to come to a very different conclusion regarding exactly how many gating cycles proceed before this tightly bound ATP dissociates.

Here, we designed a real-time ligand exchange experiment to monitor the ATP binding status in NBD1 and NBD2 during CFTR gating. For a representative experiment (Fig. 1 A; similar results were seen in nine other patches containing a single channel), a highly phosphorylated WT-CFTR channel in an excised inside-out patch was initially opened by 2.75 mM ATP (first black trace). Then, the ligand was suddenly changed (hence the name ligand exchange experiment) to 50 µM PATP, a high affinity hydrolyzable ATP analogue (Zhou et al., 2005). It can be seen that after switching the ligand from ATP to PATP, the open probability (Po) of the channel increased in two distinct steps; the channel closed time was shortened immediately (first red trace), but after an ~30-s delay, longer open time became apparent (second red trace). Fig. 1 B plots this two-step

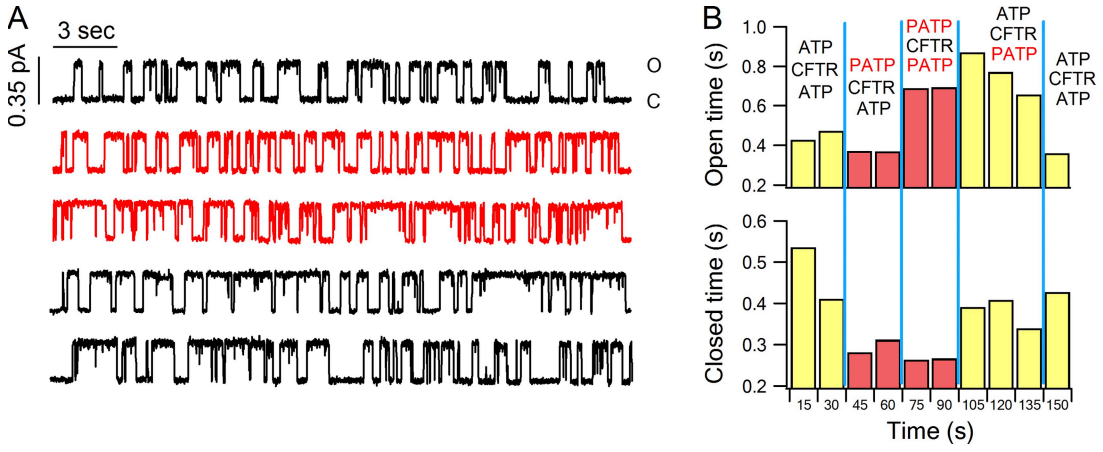

Figure 1. Changes of WT-CFTR gating kinetics upon ATP/PATP exchange. (A) A continuous single-channel current trace (a representative trace from 10 single-channel recordings) showing the effects of ligand exchanges between ATP (black traces) and PATP (red traces). (B) A history plot of the recording shown in A. Kinetic parameters were extracted with a 15-s time window. The hypothesized nucleotide binding status of CFTR at different time windows is marked.

change in channel kinetics and shows that ligand switches from PATP back to ATP also cause an immediately changed closed time and a delayed alteration of the open time.

Because single-channel data are stochastic in nature and a lengthy recording window is needed for meaningful kinetic analysis, it is difficult to accurately quantify the time course of current changes upon switching the ligand. This limitation of single-channel recordings, however, can be overcome by carrying out similar experiments in patches yielding macroscopic currents. We acquired macroscopic recordings from patches containing hundreds of WT channels. Here, changing the ligand from ATP to PATP resulted in a biphasic increase of the macroscopic current (Fig. 2 A), fit well with a double-exponential time course (red line) with a rapid ($\tau = 0.34 \pm 0.03$ s and $n = 20$) and a much slower ($\tau = 51 \pm 5$ s and $n = 19$) phase. We removed PATP and fit the subsequent current relaxations with a single-exponential function at the end of the rapid ($\tau = 0.45 \pm 0.05$ s and $n = 10$; green line) and the slow phases ($\tau = 0.79 \pm 0.04$ s and $n = 19$; blue line). Comparing the time constants of these two current decay traces with that after the withdrawal of ATP (Fig. 2 B; $\tau = 0.46 \pm 0.02$ s and $n = 25$), we found that PATP induces longer channel open time only after the appearance of the second phase. Therefore, as seen in single-channel results (Fig. 1), the application of PATP instantaneously decreases the closed time of CFTR (i.e., fast current increase) but elicits longer openings with a delay (i.e., slow current increase). It is notable that these macroscopic experiments not only confirm single-channel results shown in Fig. 1, but also provide the distinct advantage that the time course of current changes can be quantified and compared accurately.

The simplest interpretation for the results described above (see Discussion for details) is that the two NBDs have different nucleotide dwell times: ~350 ms in one NBD and ~50 s in the other NBD, based on values derived from macroscopic experiments. After changing the ligand from ATP to PATP, one NBD is immediately (in ~350 ms) vacated, allowing PATP to bind and exert its first effect rapidly (shortened closed time). However, the other NBD remains occupied by an ATP molecule for ~50 s, and therefore PATP's second effect (prolonged open time) takes place with a delay of tens of seconds (Fig. 1 B). Thus, an ATP molecule will not dissociate from CFTR for ~50 s, even when many gating cycles catalyzed by PATP in the NBD site with a fast nucleotide turnover have occurred.

The hypothesis that NBD1 is the site where ATP can bind for ~50 s during gating of CFTR appears to be more in line with what has been reported previously, including the observation that NBD1 and NBD2 assume very different catalytic ability for ATP hydrolysis (see Introduction). This hypothesis can be tested by carrying out experiments with mutations that likely perturb ATP–NBD1 interactions (e.g., Zhou et al., 2006; Tsai et al., 2009). The tryptophan residue at position 401 (W401) was chosen because the crystal structure of human NBD1 shows that the side-chain indole ring of W401 stacks against the adenine moiety of ATP (Lewis et al., 2005). When the ligand exchange experiment was performed with a single W401G channel (Fig. 3 A; similar results were seen in five other single-channel recordings), PATP (red trace) induced longer openings without an obvious delay observed with WT channels (compare Fig. 3 B with Fig. 1 B). This result was recapitulated by PATP-elicited two-step current increase (Fig. 3 C, red line) in macroscopic experiments: the first phase has a time constant of 0.32 ± 0.03 s (Fig. 3 D; $n = 11$), not different from that for WT-CFTR, but the second phase (caused by longer open time) has a time constant of 2.58 ± 0.37 s (Fig. 3 E; $n = 11$), ~20 times shorter than that observed with WT-CFTR. We interpreted these results to mean that the W401G mutation in NBD1 significantly decreases the resident time of the stably bound ATP molecule (from ~50 s for WT-CFTR to ~2.5 s for W401G-CFTR) so that PATP can replace it more rapidly and exert its second effect: increasing channel open

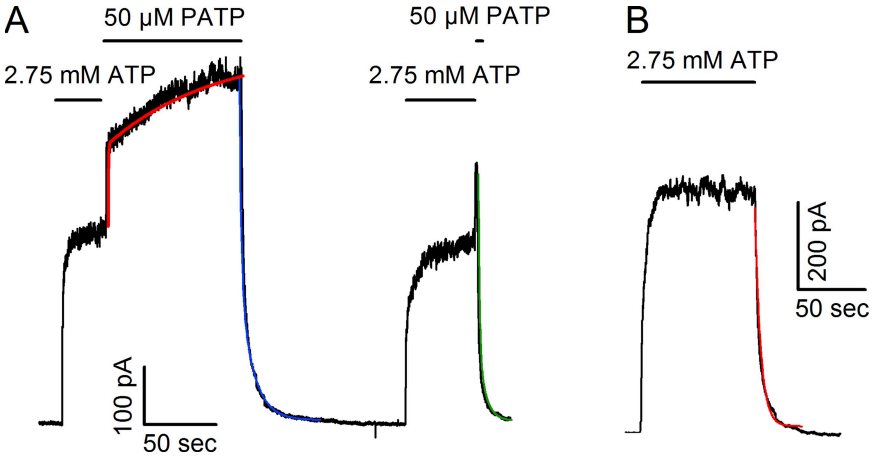

Figure 2. Changes of macroscopic WT-CFTR currents upon ATP/PATP exchange. (A) Macroscopic experiments showing a two-step current increase induced by a sudden ATP/PATP switch. PATP was removed at the end of each step. (B) Current relaxation of WT-CFTR upon removal of ATP. The current decay upon washout of ATP was fitted with a single-exponential function (red line).

time. Similar macroscopic experiments were conducted with W401I and W401Y mutations. The shorter time constant was not significantly affected by either of the mutations (Fig. 3 D), whereas the second time constant (Fig. 3 E) was shortened by nonaromatic substitutions of W401 (W401I) but increased by the conservative W401Y mutation. These results strongly support the idea that the catalysis-incapable NBD1 is the site for stable ATP binding (~50 s). It follows that rapid ATP turnover (mean nucleotide dwell time of ~350 ms) should occur in NBD2, which retains key residues for catalyzing ATP hydrolysis.

The role of NBD2's signature sequence in mediating stable ATP binding in NBD1

It was reported that the occlusion of 8-N_3 ATP in NBD1 occurs in a CFTR construct without NBD2 (Aleksandrov et al., 2008). This observation implies that it is the monomeric NBD1 that can bind ATP tightly. In contrast, functional studies (Tsai et al., 2009) suggest that stable binding of ATP occurs at the dimer interface. We now address this conflict by carrying out ligand exchange experiments with mutant channels that contain substitutions in the signature sequence of NBD2's tail subdomain, where an extensive hydrogen bond network between ATP and the signature motif is seen in structures of many ABC proteins (Fig. 4 A; also see Smith et al., 2002; Zaitseva et al., 2005). Ser 1347 (S1347) is the first candidate, as its side chain (arrow in Fig. 4 A) and the γ phosphate of ATP are close enough to form a hydrogen bond. Indeed, single S1347G channels, like W401G-CFTR (Fig. 3 A), opened into long bursts without a delay after changing the ligand from ATP to PATP (red trace in Fig. 4 B; channel kinetics summarized in Fig. 4 C), suggesting that the S1347G mutation in NBD2 dramatically shortens the dwell time of ATP in NBD1. (Similar recordings were seen in six other patches containing a single channel.) At the macroscopic level, PATP also increased the current in two phases in several S1347 mutants (two representative traces are shown in Fig. 4 D and Figs. S1 and S2). The time constants of the first phase for all S1347 mutants were similar to that of WT-CFTR (Fig. 5 A). However, the time constants of the second phase became much shorter as S1347 was altered to valine or glycine, which are incapable of forming hydrogen bonds (Fig. 5 B).

It is important to note a correlation between the degree of changes in the second time constant and the chemical nature of the mutations. As in the case for mutations at W401 (Fig. 3 E), more drastic mutations at S1347, e.g., S1347V and S1347G, shorten this time constant to a greater extent than the more conservative

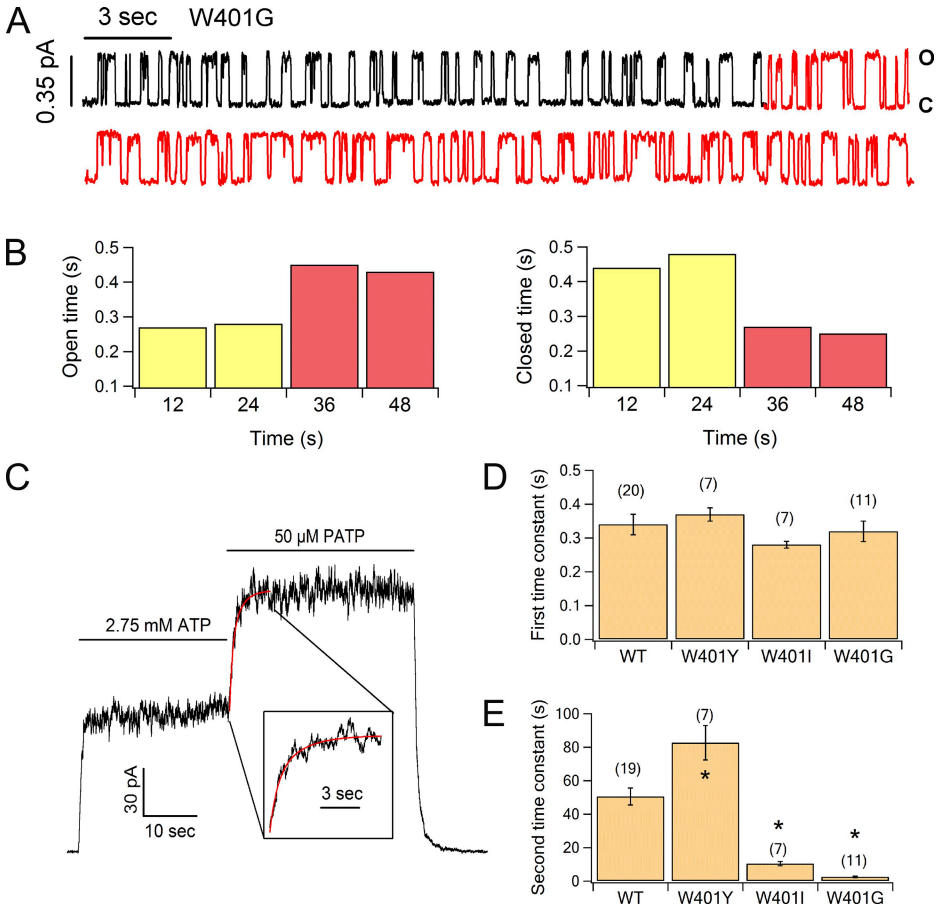

Figure 3. Effects of W401 mutations on ligand exchange. (A) The response of a single-ATP–gated W401G channel to a sudden exposure of PATP (red trace). The prolongation of the open time occurred instantly upon ligand switch. A similar observation was seen in five other patches containing a single W401G-CFTR channel. (B) Single-channel kinetics was extracted every 12 s from A. (C) Macroscopic currents recorded from hundreds of W401G channels. The current rising phase elicited by PATP was fitted with a double-exponential function (inset), yielding two time constants. (D) The fast time constants and (E) the slow time constants for WT-CFTR and different W401 mutations. *, $P < 0.01$ when compared with WT-CFTR.

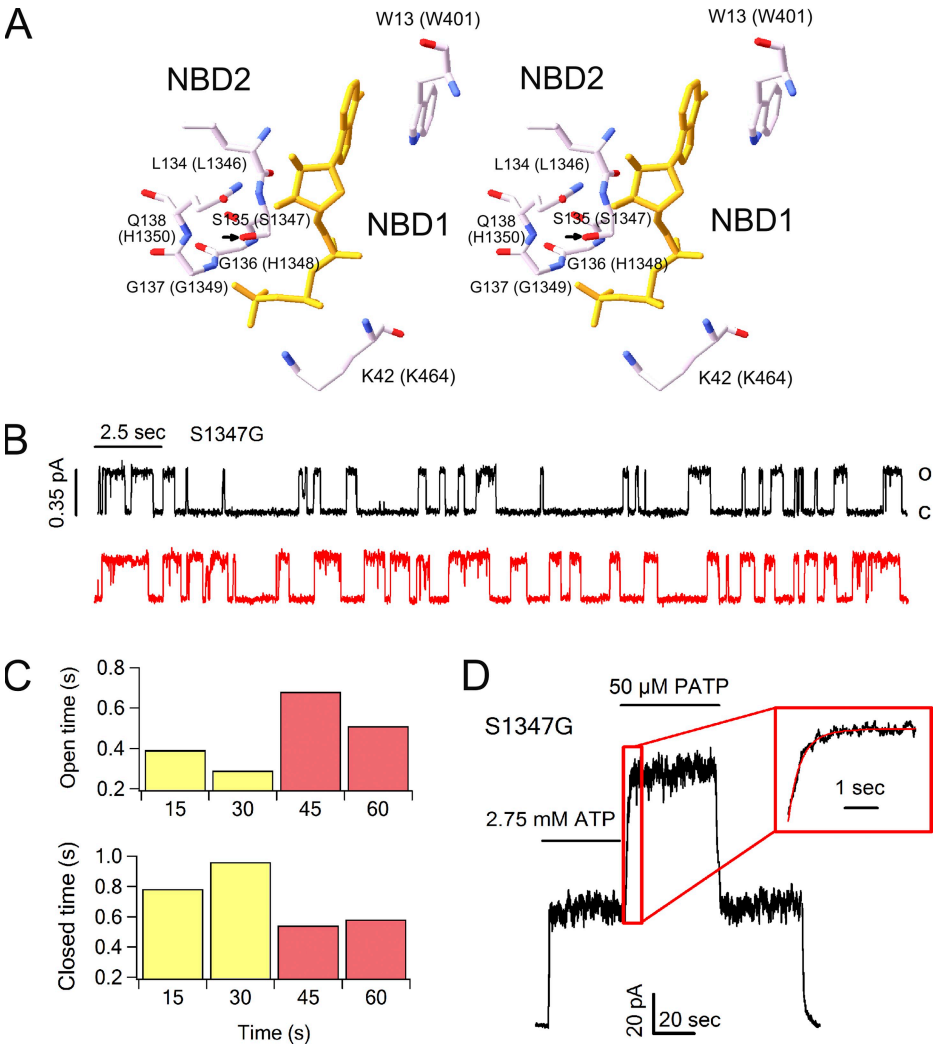

Figure 4. Effects of the S1347G mutation on ligand exchange. (A) Stereoview of interactions of ATP with key residues at the NBD dimer interface. The crystal structure of *Escherichia coli* MalK NBD dimer (Protein Data Bank accession no. 1Q12) was used to illustrate these interactions. The residue numbers in the parentheses represent the equivalent amino acids in CFTR. Arrow, the side chain of S1347. (B) A representative single S1347G-CFTR channel trace from seven similar recordings. (C) The channel entered longer openings without an obvious delay after ATP/PATP change. (D) Macroscopic currents from S1347G channels. PATP-induced current increase can be fitted well with a double-exponential function (inset).

mutation, such as S1347T (Fig. 5 B). This correlation makes it less likely that the results are due to nonspecific effects of the mutations.

We then extended our mutations to other residues in the signature sequence of the NBD2 tail. PATP induced biphasic current increase in these mutants (Figs. S1 and S2), and the time constants of the first phase were again similar to that of WT-CFTR (Fig. 5 A). The second time constant, however, was decreased by most of the mutations (Fig. 5 B). Of particular note is the H1348G mutation, which increased the time constant of the second phase (Fig. 5 B), suggesting that this mutation actually prolongs the ATP dwell time in NBD1. This result echoes typical dimeric structures of NBDs (Smith et al., 2002; Chen et al., 2003; Zaitseva et al., 2005), where the equivalent residue of H1348 is often a glycine that can interact with ATP through its backbone amide group (Fig. 4 A); thus, the presence of an imidazole ring at this position likely destabilizes ATP binding due to steric hindrance. Consistent with this idea, for the ABC protein TAP2 whose corresponding residue of H1348 is valine, a steric clash is predicted to occur as reported in a crystallographic study (Procko et al., 2006). Collectively, we conclude that both the NBD1 head and the NBD2 tail are necessary for the tight ATP binding observed in the current study.

Because different nucleotides were used in our experiments (ATP and PATP) and the photolabeling experiments (8-N_3-ATP), we wondered whether this could be the reason that biochemical occlusion can be observed even when the whole NBD2 is severed. In other words, we considered the possibility that the intrinsic high affinity of 8-N_3-ATP might be sufficient to support a tight binding of this nucleotide in NBD1 for tens of minutes independently of NBD2. To examine this possibility, we first characterized the effect of 8-N_3-ATP on WT-CFTR gating, and the results are presented in Fig. S3. In brief, compared with 2.75 mM ATP, 8-N_3-ATP at a saturating concentration (~100 μM) catalyzes the opening of WT-CFTR at an approximately two- to threefold slower rate but induces openings approximately fourfold longer, resulting in a maximal Po for channels

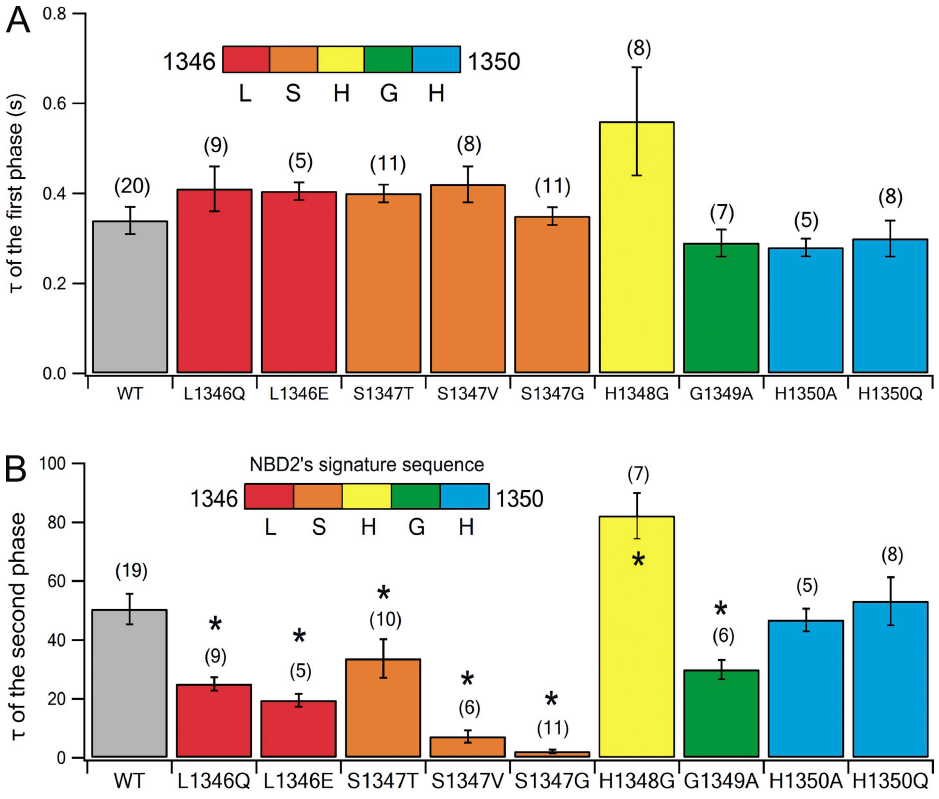

Figure 5. Time constants of the first phase (A) and the second phase (B) of the PATP-induced current increase for WT-CFTR channels and mutations in NBD2's signature sequence. Although the time constants of the first phase for all mutants tested are similar to that of WT-CFTR, the time constants for the second phase vary greatly among different mutant channels. For some mutants, the data numbers for the first and the second time constants are different. This is due to loss of the patch during recordings of the second phase. *, $P < 0.01$ when compared with WT-CFTR.

gated by 8-N_3-ATP 40% higher than that gated by ATP. These results are very similar to those reported by Basso et al. (2003).

We then asked which binding site, NBD1 or NBD2, is responsible for these differences in gating kinetics between ATP and 8-N_3-ATP. In Fig. 6 A, it can be seen that, upon a sudden solution change from 100 µM 8-N_3-ATP to 2.75 mM ATP, the macroscopic current of WT-CFTR channels decreased immediately and reached a steady state within seconds. After a continuous exposure of the channels to ATP for 60 s, ATP was removed and the time course of the current decay was fitted with a single-exponential function. The resulting time constant (red line; $\tau = 0.42 \pm 0.03$ s and $n = 4$) was not significantly different from that with only a 10-s exposure to ATP ($\tau = 0.37 \pm 0.03$ s and $n = 4$), as shown in Fig. 6 B, or that when channels were only opened by ATP without 8-N_3-ATP ($\tau = 0.34 \pm 0.03$ s and $n = 20$), as presented in Fig. 2 B. Thus, although channels gated by 8-N_3-ATP, like those by PATP, exhibit a longer open time, this effect of 8-N_3-ATP, unlike that of PATP, can be eliminated without a delay by switching the ligand to ATP. We interpret these results to mean that ATP changes the open time and the opening rate of 8-N_3-ATP–gated channels by replacing the ligand at the fast turnover site (i.e., NBD2). In other words, the differences of 8-N_3-ATP and ATP on CFTR gating are caused solely by their different effects on NBD2. It also suggests that 8-N_3-ATP and ATP exert

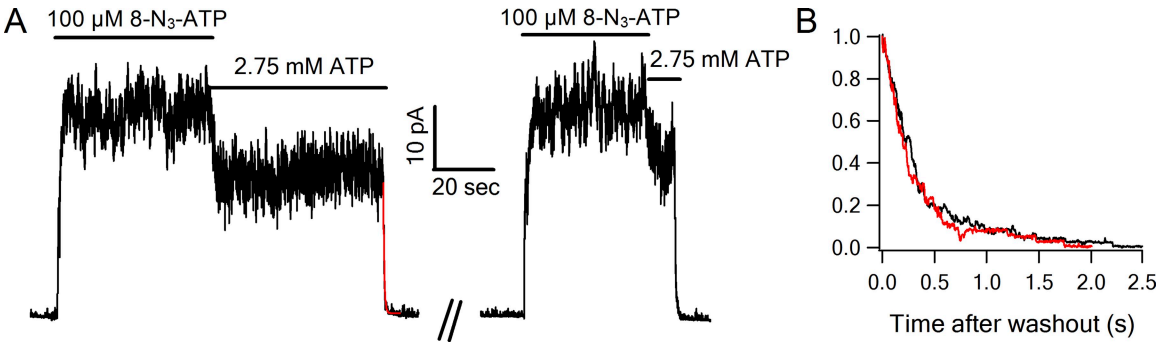

Figure 6. Changes of WT-CFTR currents upon 8-N_3-ATP/ATP exchange. (A) Macroscopic currents immediately dropped to a steady state when the solutions were switched from 8-N_3-ATP to ATP. ATP was removed either 60 or 10 s after solution changes. (B) The subsequent current relaxations were compared. Red trace, 60-s exposure to ATP; black trace, 10-s exposure to ATP.

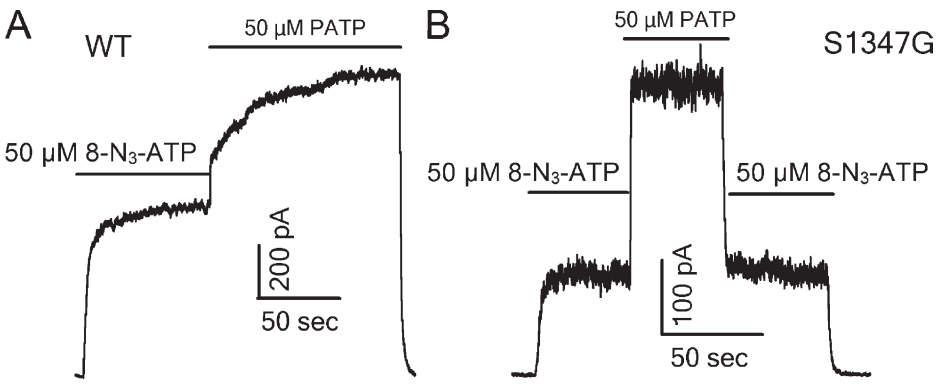

Figure 7. Changes of WT-CFTR and S1347G-CFTR currents upon 8-N_3-ATP/PATP exchange. (A) Macroscopic currents recorded from WT-CFTR channels showed a biphasic increase when 8-N_3-ATP was changed to PATP. (B) The second-phase current increase seen in A was essentially abolished by the S1347G mutation.

similar effects on gating kinetics when binding to NBD1. Indeed, as shown and explained in more detail in Fig. S4, the lock-open time with 8-N_3-ATP plus PPi is nearly identical as that with ATP plus PPi; in addition, just like ATP, 8-N_3-ATP fails to increase the activity of G551D-CFTR by binding to NBD1.

If NBD1 indeed does not differentiate 8-N_3-ATP from ATP binding, we anticipate that solution changes from 8-N_3-ATP to PATP should result in a biphasic change of macroscopic currents like those observed upon ATP/PATP exchange (Fig. 2 A) because the replacement of 8-N_3-ATP by PATP in NBD1 will similarly lead to an increased channel open time. This prediction is indeed valid, as shown in Fig. 7 A. The current rising phase upon solution changes from 8-N_3-ATP to PATP was fitted with a double-exponential function yielding two time constants ($\tau_1 = 0.81 \pm 0.17$ s and $n = 4$, and $\tau_2 = 46 \pm 6$ s and $n = 5$). The τ_1, which reflects ligand exchange in NBD2, is slightly longer than that observed in the ATP/PATP exchange experiment. This observation is expected because the turnover of 8-N_3-ATP in NBD2 is slower than that of ATP, as reflected by the longer open time seen with 8-N_3-ATP–gated channels (Fig. S3). The observation that τ_2, which represents ligand exchange in NBD1, is similar to that for ATP/PATP exchange shown in Fig. 2 A corroborates the idea that 8-N_3-ATP is trapped in NBD1 for about the same time as ATP. Furthermore, unlike the "nucleotide occlusion" phenomenon

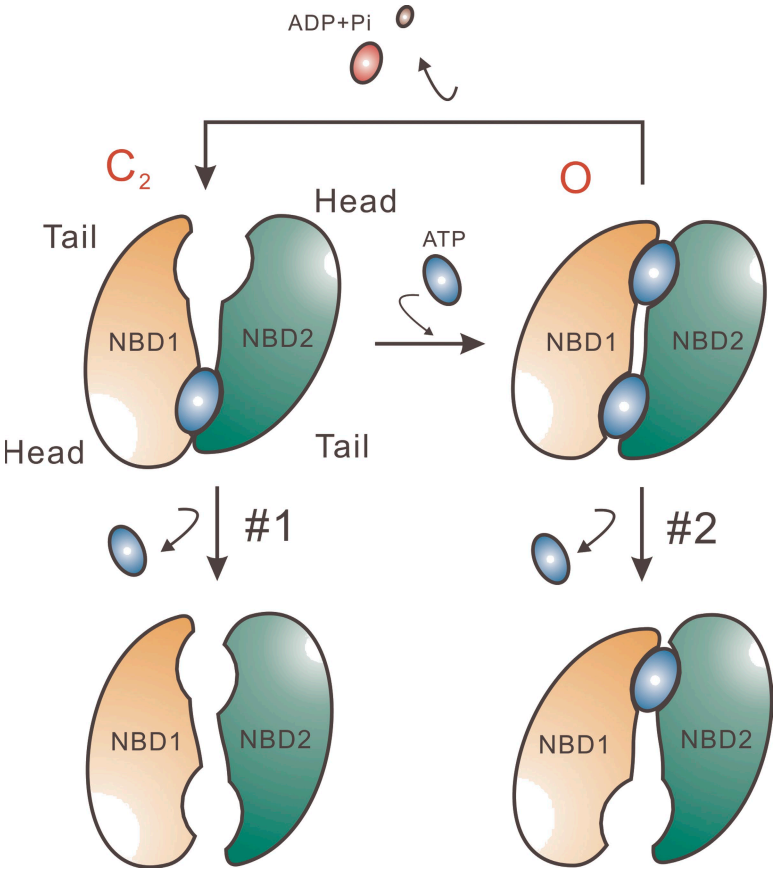

Figure 8. Diagram showing the dominant gating cycle of CFTR ($C_2 \leftrightarrow O$) and two possible pathways for the stably bound ATP molecule to dissociate.

demonstrated biochemically (Aleksandrov et al., 2008), the trapping of 8-N_3-ATP in the current study is also dependent on the tail of NBD2 because the S1347G mutation essentially abolished the second phase of current increase elicited by PATP upon switching the ligand from 8-N_3-ATP to PATP (Fig. 7 B).

Opening and closing of CFTR are coupled to the formation and partial separation of the NBD dimer

The findings described above can be interpreted in the context of the structural mechanism of CFTR gating. It is evident from the crystal structures of ABC transporters (Smith et al., 2002; Chen et al., 2003; Zaitseva, et al., 2005) that the NBDs form a dimer in a two-ATP–bound state. In CFTR, this dimeric state has been shown to represent the open state (Vergani et al., 2005; Mense et al., 2006). What remain unknown are the conformational changes of NBDs after the channel is closed by ATP hydrolysis in NBD2 (Gadsby et al., 2006; Chen and Hwang, 2008). That an ATP molecule is trapped by the NBD1 head and the NBD2 tail for ~50 s indicates that during a long period of repeated CFTR opening and closing, the NBD1 head and the NBD2 tail are kept connected by the stably bound ATP molecule. Thus, we propose that ATP hydrolysis in NBD2 brings CFTR into a partial dimer state, where the dimer interface remains partially closed to trap ATP in NBD1, allowing NBD2 to be vacated for the next ATP molecule to bind. As a result, the opening and closing of CFTR are coupled to the interconversion between a full NBD dimer (open state) and a partial NBD dimer (closed state), driven by ATP binding and hydrolysis at NBD2 ($C_2 \leftrightarrow O$ in Fig. 8).

The partial dimer state of NBDs occasionally falls into a monomeric state

Crystal structures of ABC proteins also reveal that the two NBDs rest monomerically in a nucleotide-free state (Smith et al., 2002; Chen et al., 2003; Lu et al., 2005; Zaitseva, et al., 2005). This monomeric NBD state is most likely a closed state for CFTR because CFTR rarely opens in the absence of ATP. We then ask how this state can be incorporated into the gating model proposed above. It is noted that during the slow current rising phase in Fig. 2 A, the stably bound ATP molecule in NBD1 was eventually replaced by PATP; thus, during CFTR gating, the NBD1 head and the NBD2 tail must occasionally disengage to allow ATP/PATP exchange. In theory, this separation can occur either in C_2 (#1 in Fig. 8) or O (#2 in Fig. 8) states. To distinguish between these two possibilities, we performed similar ligand exchange experiments (as Fig. 2 A) but with ATP being replaced by a lower concentration of PATP. Thus, ligand exchange in NBD1 will take place under a condition where proportionally more WT channels are in the closed (C_2) state. Fig. 9 A shows such an experiment. Upon switching ATP to 2 µM PATP, the macroscopic current changed in two phases; there was an immediate current drop followed by a slow current increase to a steady state with a time constant of 31 ± 2 s (n = 7), which is significantly shorter ($P < 0.01$) than that observed when 50 µM PATP was used (Fig. 2 A). Similar biphasic changes of the macroscopic current were also observed when ATP was switched to 5 µM PATP and the time constant of the current increase phase fell between those measured with 2 and 50 µM PATP (Fig. 9 B). These results support the notion that ATP/PATP exchange in NBD1 occurs more rapidly during the closed state (C_2). If this is indeed the case, one would predict that ATP/PATP exchange in NBD1 will take place more slowly in the open state.

Our previous studies (Tsai et al., 2009) have established that WT-CFTR can be locked open by ATP and MgPPi for ~30 s in a configuration where MgPPi binds in NBD2 while ATP occupies the NBD1 site (Fig. 10 A). Because most channels will stay in the open state when exposed to ATP and MgPPi, the subsequent solution change to PATP plus MgPPi will allow us to test whether ligand exchange in NBD1 occurs from the open state. If ATP/PATP exchange does occur in the open state (Fig. 10 B), PATP will further prolong the lock-open time because it is known that the lock-open state with MgPPi bound in NBD2 and PATP in NBD1 is more stable

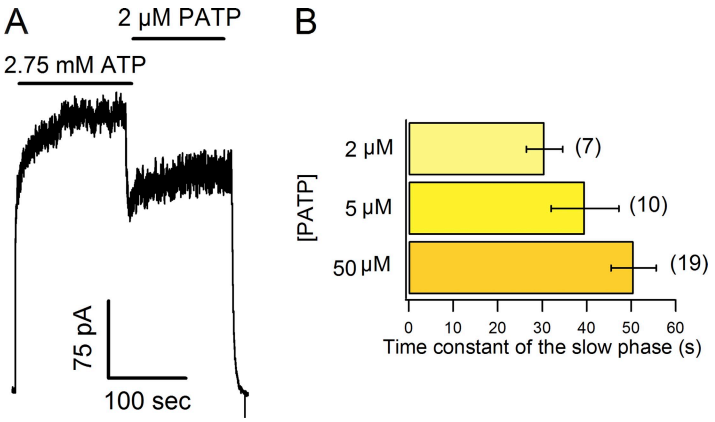

Figure 9. State dependence of ATP/PATP exchange. (A) Ligand exchange experiments with solution switches from ATP to 2 µM PATP. The macroscopic current dropped first, and then slowly increased to a steady state. (B) A bar chart comparing the time constants of the slow current increase phase when 2, 5, or 50 µM PATP was used for ligand exchange experiments.

than that with ATP in NBD1 (Tsai et al., 2009). A sample experiment is shown in Fig. 10 C. It can be seen in Fig. 10 D that 50 µM PATP plus 2 mM MgPPi (green trace) induced a more stable open state than 2.75 mM ATP plus 2 mM MgPPi (red trace) did. However, when the channels were first locked open by ATP and MgPPi, changing the solution to one containing PATP and MgPPi for even 120 s did not change the lock-open time significantly (blue trace in Fig. 10 D). In fact, a 300-s exposure to PATP and MgPPi yielded a lock-open time that is still shorter than that induced by PATP and MgPPi alone (Fig. 10 E). Fig. 10 F plots the percentage of channels with ATP/PATP exchange already occurred in NBD1 over different durations of channels' exposure to PATP and PPi, based on the assumption that the increased portion of the lock-open time (Fig. 10 E) reflects an increased percentage of channels whose NBD1 has already undergone ligand exchange (see Materials and methods). Fitting the data points with a single-exponential function (red curve in Fig. 10 F) gave a time constant of 522 s, indicating that the ATP dwell time is >10-fold longer than that measured when CFTR is not locked in the open state (Figs. 2 and 9). Thus, we conclude that during the open state (full NBD dimer state), ligand exchange in NBD1 takes place extremely slowly. These results, together with those shown in Fig. 9,

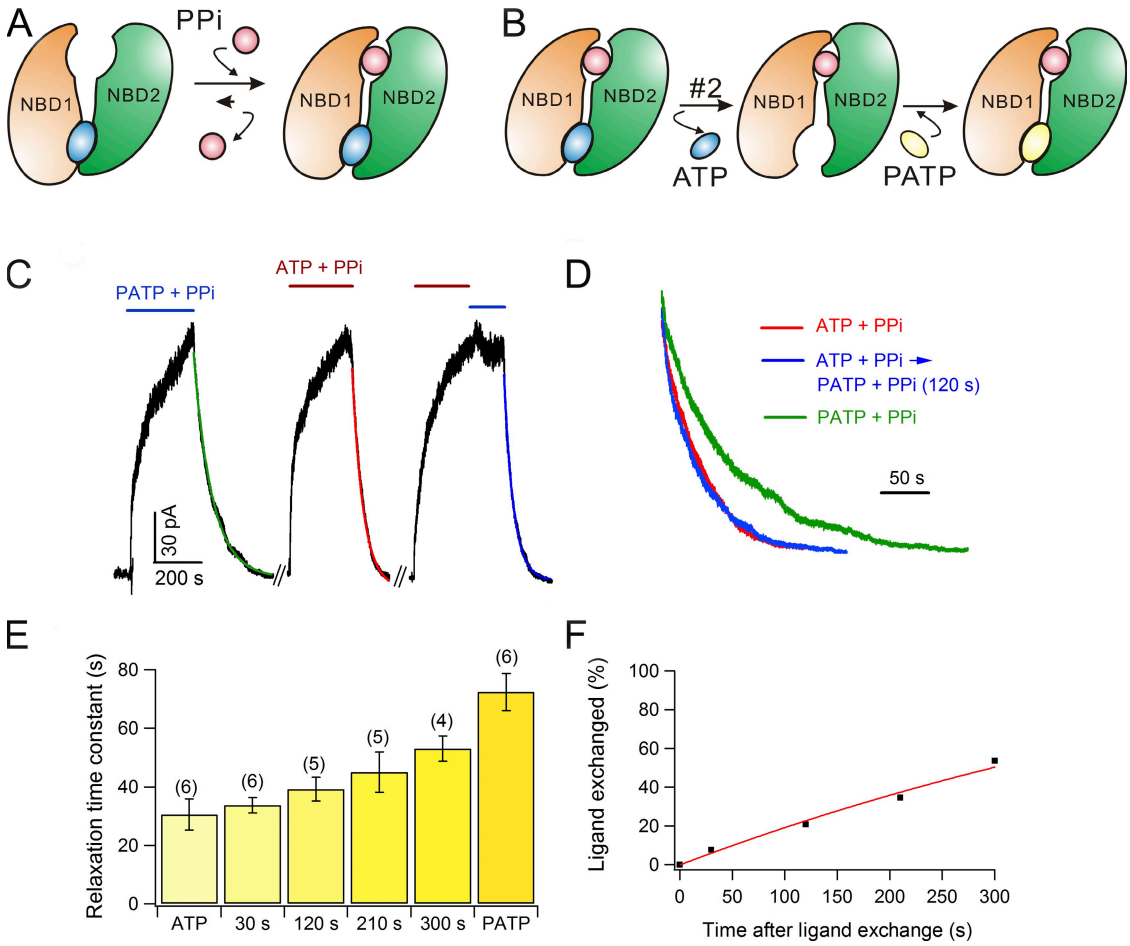

Figure 10. ATP/PATP exchange for WT-CFTR channels locked open by ATP/PATP plus PPi. (A) Cartoon illustrating the configurations of two NBDs of CFTR for the effect of PPi. The lock-open state of CFTR induced by ATP and PPi is in a configuration where ATP occupies NBD1 but PPi binds in NBD2. (B) Cartoon showing a possible ligand exchange for WT-CFTR in the lock-open state. If ATP/PATP exchange in NBD1 can occur when CFTR is locked open, the channel will enter into a more stable lock-open state where NBD1 binds a PATP molecule. (C) Current traces showing WT-CFTR channels locked into open states by ATP plus PPi, PATP plus PPi, or ATP plus PPi, followed by PATP plus PPi. The currents decayed slowly after washout. (D) A comparison for current decay traces shown in C. (E) After the application of ATP plus PPi, the longer the subsequent exposure of WT-CFTR channels to PATP plus PPi, the slower the current relaxation upon washout. (F) The current decay time constants measured under different exposure times of PATP plus PPi were converted to the proportion of channels whose ATP in NBD1 has been replaced by PATP (see Materials and methods). Data points were fitted with a single-exponential function (red curve). It is noted that because significant closed durations are expected over an experimental time span of hundreds of seconds, the resulting time constant (522 s) likely underestimates the ATP dwell time in NBD1 when CFTR is in the lock-open state. Thus, the rate of ATP/PATP exchange, ~0.002 s^{-1} (or 1/522 s), can only be considered as an upper limit for the rate of exchange for the open state.

lead us to propose that in the partial dimer state (C_2), NBD1 and NBD2 can occasionally fall apart into the monomeric resting state (i.e., $C_2 \rightarrow C_1$ in Fig. 12 A), enabling nucleotide exchange to occur in NBD1.

A second gating cycle of CFTR

We next asked after the complete disengagement of CFTR's two NBDs if the resting state can sojourn directly to the stable partial dimer state ($C_1 \rightarrow C_2$ in Fig. 12 A) before the channel opens. Alternatively, the channel must first open before a closed ATP-trapped state can form ($C_1 \rightarrow C_2' \rightarrow O \rightarrow C_2$ in Fig. 12 A). G551D, a mutation in the signature sequence of the NBD1 tail, offers an opportunity to differentiate between these two possibilities. Because this mutation eliminates ATP-dependent openings of CFTR with rare spontaneous openings left (Bompadre et al., 2007), the stable partial dimer state will not exist for G551D-CFTR if its formation requires prior ATP-induced openings ($C_1 \rightarrow C_2' \rightarrow O \rightarrow C_2$ in Fig. 12 A). Our previous studies have demonstrated that PATP increases the Po of G551D channels by binding to NBD1, whereas it exerts no effects when binding to NBD2 (Bompadre et al., 2008). Thus, the time course of current rise upon ATP/PATP switch will reflect the dissociation rate of ATP from NBD1 of G551D-CFTR. In the current trace shown in Fig. 11, after ligand changes from ATP to PATP, the rapid monophasic ($\tau = 2.1 \pm 0.3$ s and $n = 11$) increase of G551D currents indicates that unlike WT channels, ATP is not stably trapped in the NBD1 of G551D-CFTR. In other words, the binding of ATP in G551D-CFTR's NBD1 does not lead to a stable partial dimer state. Thus, we propose that the disassembly of the partial NBD dimer ($C_2 \rightarrow C_1$ in Fig. 12 A) is a poorly reversible process. The implication for this proposition is that the channel in the resting state has to open first before a closed ATP-trapped partial dimer state can form ($C_1 \rightarrow C_2' \rightarrow O \rightarrow C_2$ in Fig. 12 A). That is, the channel in the monomeric state enters into the open state through a second gating cycle, distinct from the dominant gating cycle discussed above ($C_2 \leftrightarrow O$ in Fig. 12 A).

We noticed that an alternative interpretation of the results shown in Fig. 11 is that ATP binding to NBD1 can bring the channel into the partial dimer state (i.e., the step C_1 to C_2 is readily reversible), but the partial dimer state is so severely destabilized that the NBD1 site can be loaded by PATP rapidly after ligand exchange. In this scenario, the G551D mutation in the helical subdomain of NBD1 has to allosterically affect tight nucleotide binding observed in NBD1's core subdomain in spite of >10-Å distance in between (Lewis et al., 2004, 2005). One possibility to envision such allosteric communication

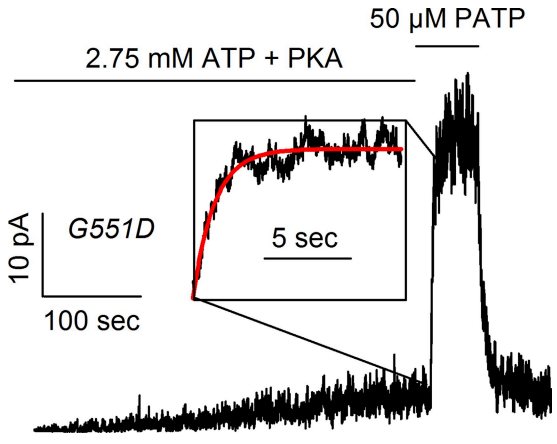

Figure 11. Ligand exchange experiments conducted with G551-CFTR. The G551D mutant channels were activated by PKA and ATP to a steady state before the solution was changed to one containing PATP. The macroscopic current increased monotonically (inset) by PATP, although G551D-CFTR did not respond to ATP.

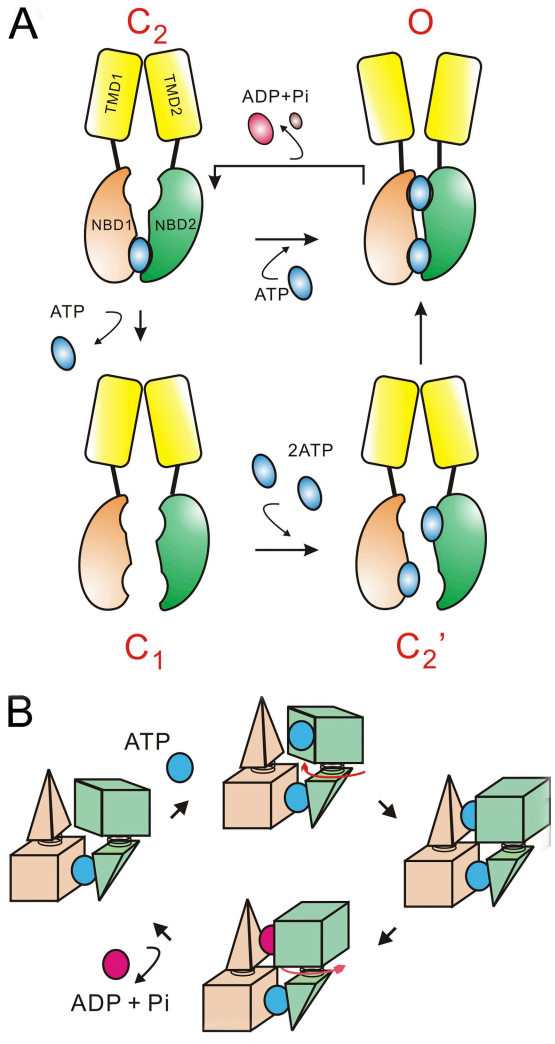

Figure 12. Molecular model of CFTR gating. (A) A simplified diagram illustrating dominant gating transitions ($C_2 \leftrightarrow O$) and a second gating cycle ($C_1 \rightarrow C_2' \rightarrow O \rightarrow C_2 \rightarrow C_1$) involving complete disengagement of the two NBDs. (B) A proposed mechanism for partial separation and reformation of the NBD dimer. Cubes, head subdomains of NBDs; pyramids, tail subdomains of NBDs.

is that the negatively charged D551 side chain could somehow clash with the ATP or PATP molecule bound in the head of NBD2, pushing the two NBDs away from each other. However, in Figs. S5 and S6, we show that this is unlikely the case because introducing the Y1219G mutation, which greatly disrupts ATP or PATP binding in NBD2 (Fig. S5), into the G551D background does not significantly (P = 0.78) alter the time constant of current increase upon ATP/PATP switch (Fig. S6). We acknowledge that we cannot test and rule out all possible allosteric mechanisms, but our proposition of the irreversibility of the $C_2 \rightarrow C_1$ step is at least consistent with two lines of structural/functional observations as detailed in the Discussion.

DISCUSSION

In this, we designed a novel ligand exchange protocol to investigate the ATP binding status in CFTR's two NBDs. The results led us to propose that an ATP molecule stays in NBD1 for tens of seconds, spanning many gating cycles of CFTR, and that this stably bound ATP molecule is trapped by the NBD1 head and the NBD2 tail at the dimer interface. Based on findings in the current studies as well as those in the literature, we can establish a molecular mechanism for CFTR gating by its two NBDs. We posit that the dominant gating cycle of CFTR represents a repeated interconversion between the full NBD dimer and the partial dimer state ($C_2 \leftrightarrow O$ in Fig. 12 A). We also present evidence for a second gating cycle, which involves a poorly reversible process of partial dimer separation into the rarely existed monomeric NBD state ($O \rightarrow C_2 \rightarrow C_1 \rightarrow C_2' \rightarrow O$ in Fig. 12 A).

Stable nucleotide binding in NBD1 and the underlying structural mechanism

Our ATP/PATP exchange experiments to investigate ATP binding status in CFTR's NBDs led to several conclusions generally consistent with our previous work (Tsai et al., 2009) that used an independent experimental strategy. On the other hand, our conclusions are qualitatively and quantitatively different from those of photolabeling experiments (Basso et al., 2003; Aleksandrov et al., 2008) because the stable ATP binding in NBD1 demonstrated here was ~50-fold less stable than the biochemically observed 8-N_3-ATP occlusion, and because in our study the signature sequence of NBD2 plays a key role for ATP to bind tightly in NBD1.

Before we discuss possible explanations for these discrepancies, however, we first acknowledge that the limitation of our functional approach is that, unlike photolabeling experiments, it does not allow us to "see" directly the bound ATP molecules in CFTR. Instead, our direct experimental observations were that upon ATP/PATP exchange, one of the gating properties with ATP (shorter open time than that induced by PATP) can last for ~50 s, as if the channel can remember its history of being gated by ATP even after the ligand has been replaced by PATP for ~50 s. This long-lasting "memory" can be explained by a simple idea that an ATP molecule can physically bind in the CFTR protein for tens of seconds without dissociation, so that the shorter open time of ATP-gated CFTR can be maintained. We realized that there are alternative explanations for this long-lasting effect of ATP. For example, one can argue that ATP may dissociate immediately once the ATP-containing solution is changed, but the ATP-induced conformational changes can persist for tens of seconds. In other words, it is not the ATP binding per se but the relaxation of the conformational changes that takes a long time to complete. However, our observation that nonconservative mutations at W401, a residue that interacts with ATP in the crystal structure of CFTR's NBD1 (Lewis et al., 2005), greatly accelerated the dissipation of ATP's long-lasting effects on channel open time after ATP/PATP exchange (Fig. 3) strongly suggests that this long-lasting remembrance of the gating history is due to a physically bound ATP molecule that stays in the CFTR protein for tens of seconds.

The results that mutations in either the W401 residue or in the signature sequence of NBD2 modulate how long ATP's effect on CFTR open time can last (or how long the delay is for PATP to catalyze long openings) suggest that the stable ATP binding occurs at the interface between the NBD1 head and the NBD2 tail. It should be noted that these mutational effects are relatively specific because we observed a correlation between the chemical nature of the mutations and the degree of perturbations (Figs. 3–5), and also because all these mutations mostly affect the second kinetic change (i.e., changes in the open time) after ligand switches and bear little influence on the first step (i.e., changes in the closed time) (Fig. 5). The proposition that a tightly bound ATP molecule in NBD1 prevents PATP from inducing long CFTR openings also corroborates previous reports that PATP affects the open-state stability by its interactions with NBD1 (Zhou et al., 2005, 2006; Tsai et al., 2009).

The exact reason for the aforementioned discrepancy between our functional data and biochemical studies (Basso et al., 2003; Aleksandrov et al., 2008) is unclear. We can, however, at least argue that the difference in the ligand used in these two sets of experiments is unlikely the culprit because our data suggest that 8-N_3-ATP is trapped at the dimer interface for a nearly identical time as ATP. One may simply speculate that in the membrane preparation used for photolabeling experiments and in excised inside-out membrane patches, CFTR proteins adopt different tertiary structures and thus have distinct structural mechanisms for retaining nucleotides in NBD1. We reasoned that a more likely

scenario to explain the discrepancy lies in the fact that not all CFTR proteins in the cell are mature and functional. Because only functional channels yield currents in electrophysiological recordings, our approach inevitably targets only functional CFTR proteins residing in the plasma membrane.

Two gating cycles of CFTR channels

In the Results, we proposed that the primary mode of CFTR's opening–closing cycle represents a repeated switch between a full NBD dimer (open state; Vergani et al., 2005) and a partial NBD dimer (closed state; $C_2 \leftrightarrow O$ in Fig. 12 A). During these gating cycles, the NBD1 head and the NBD2 tail are connected so as to retain an ATP molecule at the NBD interface for tens of seconds. A model with a similar molecular picture has been proposed before (Gadsby et al., 2006), based on the assumption that biochemically demonstrated nucleotide occlusion in NBD1 occurs at the NBD dimer interface. However, the validity of this assumption has been undermined by a similar occlusion phenomenon observed with ΔNBD2-CFTR (Aleksandrov et al., 2008).

Crystallographic studies of the ABC proteins have provided a clue for how partial separation of an NBD dimer could be achieved. It has been demonstrated that compared with the ATP-free form, the ATP-bound monomeric NBD shows a rigid-body rotation of the helical subdomain relative to the core subdomain for over 10 degrees (Karpowich et al., 2001; Yuan et al., 2001; Smith et al., 2002; Chen et al., 2003; Zaitseva et al., 2005), moving the NBDs into a dimerization-favoring orientation, where the helical subdomain from one NBD now faces the ATP binding site in the core subdomain of the partner NBD. It was also thought that upon ATP hydrolysis, a reverse rotation happens to expose the ATP binding site to facilitate nucleotide exchange (Karpowich et al., 2001). We propose that similar rotational movements of CFTR's NBD2, induced by ATP binding and hydrolysis, may also open and close the interface between CFTR's NBD2 head and the NBD1 tail (Fig. 12 B). These "limited" molecular motions may constitute the fundamental mechanism by which NBDs control the CFTR gate.

For the other binding site, where ATP is not hydrolyzed but trapped at the dimer interface, dissociation of the tightly bound ATP molecule likely requires some degree of separation of the NBD1 head and the NBD2 tail. Interestingly, our data (Figs. 8–10) suggest that this occurs more readily when CFTR is in the partial dimer state than in the full dimer state. Thus, it appears that the closing of the dimer interface between the head of NBD2 and the tail of NBD1 can somehow stabilize the other interface formed by the head of NBD1 and the tail of NBD2, indicating an allosteric communication mechanism. This communication is likely bidirectional because it has also been demonstrated that a tighter binding of nucleotides at the dimer interface between the head of NBD1 and the tail of NBD2 slows down channel closure (Zhou et al., 2005), which represents the separation of the interface between the NBD2 head and the NBD1 tail. It is noted that our observation of allosteric interactions between the two interfaces again contradicts results from photolabeling experiments where nucleotide occlusion in NBD1 was not affected by mutations of the conserved lysine (K1250) residue in NBD2, and ATP binding at NBD2 was also unaffected by mutations of the equivalent residue (K464) in NBD1 (Aleksandrov et al., 2002).

The finding that G551D-CFTR, unlike WT channels, does not trap ATP in NBD1 (Fig. 11) was interpreted to mean that the disassembly of the stable partial NBD dimer ($C_2 \rightarrow C_1$ in Fig. 12 A) is a poorly reversible process. That is, ATP binding in NBD1 is insufficient to induce a stable partial NBD dimer (see also Results). We realized that even though we have conducted some control experiments (Figs. S5 and S6), it remains virtually impossible for us to exclude the possibility that this observation is due to a nonspecific mutational effect on the stability of the C_2 state as elaborated in the Results. However, we should point out that our proposition is at least consistent with some structural data in the literature. First, the crystal structure of mouse CFTR's NBD1 shows little conformational difference between nucleotide-free, ADP-, or ATP-bound forms (Lewis et al., 2004), as opposed to the NBDs of many other ABC proteins (Karpowich et al., 2001; Yuan et al., 2001; Smith et al., 2002; Chen et al., 2003; Zaitseva et al., 2005). Thus, ATP binding in NBD1 may not induce necessary conformational changes thought to favor NBD dimerization. Second, an evolutionarily conserved hydrogen bond pair critical for NBD dimerization (Vergani et al., 2005) was only found in the NBD2 head (R555) and the NBD1 tail (T1246). The corresponding residues in the NBD1 head and the NBD2 tail cannot form a hydrogen bond. Therefore, in the resting state, the energy barrier to form a stable partial dimer state ($C_1 \rightarrow C_2$) may be much higher than that for the resting state to enter the open state ($C_1 \rightarrow C_2' \rightarrow O$) where the transition state may be stabilized by the hydrogen bond (R555-T1246) at the dimer interface.

If the aforementioned argument made for the G551D-CFTR is also valid for WT-CFTR, when WT channels occasionally exit from the primary gating cycle ($C_2 \leftrightarrow O$) through a rare separation of the partial dimer ($C_2 \rightarrow C_1$), the channel, now in the monomeric NBD state, will reenter the open state via a distinct opening pathway, during which ATP binding in NBD1 is relatively unstable. This process represents a second gating cycle for CFTR ($O \rightarrow C_2 \rightarrow C_1 \rightarrow C_2' \rightarrow O$). The dynamic interaction between two NBDs during the transition from the monomeric state to the dimeric state ($C_1 \rightarrow C_2' \rightarrow O$) is unclear and awaiting more thorough investigations. We speculate that ATP binding to the head of monomeric

NBD2 may recruit the NBD1 tail, initiating a closure of the dimer interface. We envision that this molecular motion then proceeds to completion by including the ATP molecule in NBD1 and thus leads to a stabilized ATP binding there.

The structural/functional implications for other ABC proteins

The molecular model (Fig. 12) we proposed here also poses several structural and functional implications for other ABC proteins. First, although the separation of the NBD dimer from the two-ATP–bound state to the nucleotide-free state is evident from crystal structures of ABC transporters, it is unclear whether hydrolysis of one ATP molecule is sufficient to open an NBD dimer (discussed in van der Does and Tampé, 2004; Oswald et al., 2006; Sauna et al., 2007; Davidson et al., 2008; Procko et al., 2009). To directly address this issue, it is necessary to characterize a single-ATP–bound state of NBDs. However, isolating such an intermediate state has proven difficult for experimental approaches to date. Molecular dynamic simulations may provide help to understand its structural properties, but the results from different groups are contradictory (Wen and Tajkhorshid, 2008; Jones and George, 2009). In the current study, we demonstrated that after hydrolysis of one ATP molecule, the NBD dimer, at least for CFTR, can remain partially connected by the remaining ATP molecule (i.e., partial dimer state). Although the detailed 3-D structure of the partial dimer state is unknown, we believe that crystallization of NBDs in this state can be attained by mutating catalytic residues in only one of an ABC protein's two NBDs, mimicking the asymmetric catalytic ability of CFTR's NBDs.

How the function of ABC proteins is supported by ATP binding and hydrolysis events that occurred in NBDs has received great attention in the ABC protein field. Recent advances in solving the structures of full-length ABC transporters have revealed that the TMDs of these proteins adopt inward- and outward-facing conformations, respectively, when the NBDs are in the ATP-free monomeric and two-ATP–bound dimeric forms (for example, Ward et al., 2007; Aller et al., 2009; Khare et al., 2009). Thus, the opening and closing of the NBD dimer interface appears to drive the "alternating access" (Jardetzky, 1966) of the substance binding site located in the TMDs, so that the cargo can bind from one side of the membrane and be released from the other side, fulfilling the structural requirement of an active transporter. A structure-based model has therefore emerged, with the function of ABC proteins being coupled to the "large-scale" movements of repeated formation and separation of the NBD dimer (for review see Hollenstein et al., 2007; Oldham et al., 2008; Rees et al., 2009). However, this model overlooks the single-ATP–bound state discussed above.

Because the NBDs seldom disengage completely for many CFTR gating cycles, we propose that, unlike the structure-based model, "limited motions" of NBDs (i.e., partial separation and reformation) are sufficient to complete a cycle of conformational changes in TMDs for CFTR. For many asymmetric ABC proteins such as human multiple drug–resistant protein 1 or sulfonylurea receptor, their NBD1, similar to CFTR, also has substitutions in key catalytic residues and thus displays a stable ATP binding phenomenon (Matsuo et al., 1999, 2000; Ueda et al., 1999; Gao et al., 2000; Hou et al., 2000; Nagata et al., 2000). If the duration of their functional cycle is substantially shorter than the ATP dwell time in NBD1, and if the tight ATP binding is also mediated by a partial dimer state, one has to conclude that limited movements of NBDs can also be sufficient to support the function of these asymmetric ABC proteins.

For ABC proteins with two catalysis-competent sites, the stoichiometry of ATP hydrolysis per functional cycle has been under intense debates. The "sequential hydrolysis" or "processive clamp" model suggests that hydrolysis of two ATP molecules is necessary for a single functional cycle (Janas et al., 2003), thus inferring that a functional cycle involves a complete separation of the NBD dimer. This mechanism appears to gain supports from crystallographic studies, as no structure so far is solved in a single-ATP–bound form. On the other hand, an "alternating catalytic sites" model was proposed for human P-glycoproteins (Urbatsch et al., 1995; Tombline et al., 2004) and *Escherichia coli* maltose transporters (Sharma and Davidson, 2000), suggesting that only one ATP molecule is hydrolyzed in a transport cycle. Our proposition of limited NBD motions between a full NBD dimer and a single-ATP–bound partial dimer provides support for this latter model. In fact, based on the crystal structure of Sav1866, a bacterial ABC protein with both NBDs capable of catalyzing ATP hydrolysis, it was argued that the motion of NBDs is restrained by TMDs and thus probably cannot carry out large movements as suggested by the aforementioned structure-based model (Schuldiner, 2006).

Potential applications of ligand exchange experiments

In addition to tracing ATP binding in CFTR's NBDs, the ligand exchange experiments developed here can also be a powerful tool to investigate how different nucleotide ligands affect CFTR's function. Upon solution switches from ATP to a second ligand, because one ATP can stay bound in NBD1 for ~50 s, an immediate change of CFTR's gating kinetics is caused by the binding of the second ligand to NBD2. It follows that if the ligand can exert some effects on CFTR's function by binding to NBD1, this effect will occur only after an ~50-s delay. Using this method, we have found that 8-N_3-ATP induces a slower opening rate but a longer open time

than ATP simply because of its different interactions with CFTR's NBD2 (Figs. 6 and 7, and Figs. S3 and S4). On the other hand, PATP catalyzes fast channel openings by binding to NBD2 but long open bursts by interacting with NBD1. CFTR can be opened by a wide range of nucleotide triphosphates other than ATP, including GTP, UTP, ITP, CTP, and AMP-CPP (Anderson et al., 1991). Comparing the mechanism of these ligands' influence on CFTR gating may represent an opportunity for a better understanding of ligand–NBD interactions in the future.

We thank Dr. Chris Miller, Tsung-Yu Chen, and Kevin Gillis for helpful discussion of the manuscript and Cindy Chu for technical assistance.

This work was supported by National Institutes of Health grants R01HL53445 and R01DK55835 to T.-C. Hwang.

Angus C. Nairn served as editor.

Submitted: 4 January 2010
Accepted: 8 April 2010

REFERENCES

Aleksandrov, L., A.A. Aleksandrov, X.B. Chang, and J.R. Riordan. 2002. The first nucleotide binding domain of cystic fibrosis transmembrane conductance regulator is a site of stable nucleotide interaction, whereas the second is a site of rapid turnover. *J. Biol. Chem.* 277:15419–15425. doi:10.1074/jbc.M111713200

Aleksandrov, L., A. Aleksandrov, and J.R. Riordan. 2008. Mg2+-dependent ATP occlusion at the first nucleotide-binding domain (NBD1) of CFTR does not require the second (NBD2). *Biochem. J.* 416:129–136. doi:10.1042/BJ20081068

Aller, S.G., J. Yu, A. Ward, Y. Weng, S. Chittaboina, R. Zhuo, P.M. Harrell, Y.T. Trinh, Q. Zhang, I.L. Urbatsch, and G. Chang. 2009. Structure of P-glycoprotein reveals a molecular basis for poly-specific drug binding. *Science.* 323:1718–1722. doi:10.1126/science.1168750

Anderson, M.P., H.A. Berger, D.P. Rich, R.J. Gregory, A.E. Smith, and M.J. Welsh. 1991. Nucleoside triphosphates are required to open the CFTR chloride channel. *Cell.* 67:775–784. doi:10.1016/0092-8674(91)90072-7

Basso, C., P. Vergani, A.C. Nairn, and D.C. Gadsby. 2003. Prolonged nonhydrolytic interaction of nucleotide with CFTR's NH_2-terminal nucleotide binding domain and its role in channel gating. *J. Gen. Physiol.* 122:333–348. doi:10.1085/jgp.200308798

Bear, C.E., C.H. Li, N. Kartner, R.J. Bridges, T.J. Jensen, M. Ramjeesingh, and J.R. Riordan. 1992. Purification and functional reconstitution of the cystic fibrosis transmembrane conductance regulator (CFTR). *Cell.* 68:809–818. doi:10.1016/0092-8674(92)90155-6

Bompadre, S.G., T. Ai, J.H. Cho, X. Wang, Y. Sohma, M. Li, and T.C. Hwang. 2005. CFTR gating I. Characterization of the ATP-dependent gating of a phosphorylation-independent CFTR channel (ΔR-CFTR). *J. Gen. Physiol.* 125:361–375. doi:10.1085/jgp.200409227

Bompadre, S.G., Y. Sohma, M. Li, and T.C. Hwang. 2007. G551D and G1349D, two CF-associated mutations in the signature sequences of CFTR, exhibit distinct gating defects. *J. Gen. Physiol.* 129:285–298. doi:10.1085/jgp.200609667

Bompadre, S.G., M. Li, and T.C. Hwang. 2008. Mechanism of G551D-CFTR (cystic fibrosis transmembrane conductance regulator) potentiation by a high affinity ATP analog. *J. Biol. Chem.* 283:5364–5369. doi:10.1074/jbc.M709417200

Chen, J., G. Lu, J. Lin, A.L. Davidson, and F.A. Quiocho. 2003. A tweezers-like motion of the ATP-binding cassette dimer in an ABC transport cycle. *Mol. Cell.* 12:651–661. doi:10.1016/j.molcel.2003.08.004

Chen, T.Y., and T.C. Hwang. 2008. CLC-0 and CFTR: chloride channels evolved from transporters. *Physiol. Rev.* 88:351–387. doi:10.1152/physrev.00058.2006

Csanády, L. 2000. Rapid kinetic analysis of multichannel records by a simultaneous fit to all dwell-time histograms. *Biophys. J.* 78:785–799. doi:10.1016/S0006-3495(00)76636-7

Davidson, A.L., and J. Chen. 2004. ATP-binding cassette transporters in bacteria. *Annu. Rev. Biochem.* 73:241–268. doi:10.1146/annurev.biochem.73.011303.073626

Davidson, A.L., E. Dassa, C. Orelle, and J. Chen. 2008. Structure, function, and evolution of bacterial ATP-binding cassette systems. *Microbiol. Mol. Biol. Rev.* 72:317–364. doi:10.1128/MMBR.00031-07

Gadsby, D.C., P. Vergani, and L. Csanády. 2006. The ABC protein turned chloride channel whose failure causes cystic fibrosis. *Nature.* 440:477–483. doi:10.1038/nature04712

Gao, M., H.R. Cui, D.W. Loe, C.E. Grant, K.C. Almquist, S.P. Cole, and R.G. Deeley. 2000. Comparison of the functional characteristics of the nucleotide binding domains of multidrug resistance protein 1. *J. Biol. Chem.* 275:13098–13108. doi:10.1074/jbc.275.17.13098

Hollenstein, K., R.J. Dawson, and K.P. Locher. 2007. Structure and mechanism of ABC transporter proteins. *Curr. Opin. Struct. Biol.* 17:412–418. doi:10.1016/j.sbi.2007.07.003

Hou, Y., L. Cui, J.R. Riordan, and X. Chang. 2000. Allosteric interactions between the two non-equivalent nucleotide binding domains of multidrug resistance protein MRP1. *J. Biol. Chem.* 275:20280–20287. doi:10.1074/jbc.M001109200

Janas, E., M. Hofacker, M. Chen, S. Gompf, C. van der Does, and R. Tampé. 2003. The ATP hydrolysis cycle of the nucleotide-binding domain of the mitochondrial ATP-binding cassette transporter Mdl1p. *J. Biol. Chem.* 278:26862–26869. doi:10.1074/jbc.M301227200

Jardetzky, O. 1966. Simple allosteric model for membrane pumps. *Nature.* 211:969–970. doi:10.1038/211969a0

Jones, P.M., and A.M. George. 2009. Opening of the ADP-bound active site in the ABC transporter ATPase dimer: evidence for a constant contact, alternating sites model for the catalytic cycle. *Proteins.* 75:387–396. doi:10.1002/prot.22250

Karpowich, N., O. Martsinkevich, L. Millen, Y.R. Yuan, P.L. Dai, K. MacVey, P.J. Thomas, and J.F. Hunt. 2001. Crystal structures of the MJ1267 ATP binding cassette reveal an induced-fit effect at the ATPase active site of an ABC transporter. *Structure.* 9:571–586. doi:10.1016/S0969-2126(01)00617-7

Khare, D., M.L. Oldham, C. Orelle, A.L. Davidson, and J. Chen. 2009. Alternating access in maltose transporter mediated by rigid-body rotations. *Mol. Cell.* 33:528–536. doi:10.1016/j.molcel.2009.01.035

Lewis, H.A., S.G. Buchanan, S.K. Burley, K. Conners, M. Dickey, M. Dorwart, R. Fowler, X. Gao, W.B. Guggino, W.A. Hendrickson, et al. 2004. Structure of nucleotide-binding domain 1 of the cystic fibrosis transmembrane conductance regulator. *EMBO J.* 23:282–293. doi:10.1038/sj.emboj.7600040

Lewis, H.A., X. Zhao, C. Wang, J.M. Sauder, I. Rooney, B.W. Noland, D. Lorimer, M.C. Kearins, K. Conners, B. Condon, et al. 2005. Impact of the deltaF508 mutation in first nucleotide-binding domain of human cystic fibrosis transmembrane conductance regulator on domain folding and structure. *J. Biol. Chem.* 280:1346–1353. doi:10.1074/jbc.M410968200

Lu, G., J.M. Westbrooks, A.L. Davidson, and J. Chen. 2005. ATP hydrolysis is required to reset the ATP-binding cassette dimer

into the resting-state conformation. *Proc. Natl. Acad. Sci. USA.* 102:17969–17974. doi:10.1073/pnas.0506039102

Matsuo, M., N. Kioka, T. Amachi, and K. Ueda. 1999. ATP binding properties of the nucleotide-binding folds of SUR1. *J. Biol. Chem.* 274:37479–37482. doi:10.1074/jbc.274.52.37479

Matsuo, M., K. Tanabe, N. Kioka, T. Amachi, and K. Ueda. 2000. Different binding properties and affinities for ATP and ADP among sulfonylurea receptor subtypes, SUR1, SUR2A, and SUR2B. *J. Biol. Chem.* 275:28757–28763. doi:10.1074/jbc.M004818200

Mense, M., P. Vergani, D.M. White, G. Altberg, A.C. Nairn, and D.C. Gadsby. 2006. In vivo phosphorylation of CFTR promotes formation of a nucleotide-binding domain heterodimer. *EMBO J.* 25:4728–4739. doi:10.1038/sj.emboj.7601373

Nagata, K., M. Nishitani, M. Matsuo, N. Kioka, T. Amachi, and K. Ueda. 2000. Nonequivalent nucleotide trapping in the two nucleotide binding folds of the human multidrug resistance protein MRP1. *J. Biol. Chem.* 275:17626–17630. doi:10.1074/jbc.M000792200

Oldham, M.L., A.L. Davidson, and J. Chen. 2008. Structural insights into ABC transporter mechanism. *Curr. Opin. Struct. Biol.* 18:726–733. doi:10.1016/j.sbi.2008.09.007

Oswald, C., I.B. Holland, and L. Schmitt. 2006. The motor domains of ABC-transporters. What can structures tell us? *Naunyn Schmiedebergs Arch. Pharmacol.* 372:385–399. doi:10.1007/s00210-005-0031-4

Procko, E., I. Ferrin-O'Connell, S.L. Ng, and R. Gaudet. 2006. Distinct structural and functional properties of the ATPase sites in an asymmetric ABC transporter. *Mol. Cell.* 24:51–62. doi:10.1016/j.molcel.2006.07.034

Procko, E., M.L. O'Mara, W.F. Bennett, D.P. Tieleman, and R. Gaudet. 2009. The mechanism of ABC transporters: general lessons from structural and functional studies of an antigenic peptide transporter. *FASEB J.* 23:1287–1302. doi:10.1096/fj.08-121855

Rees, D.C., E. Johnson, and O. Lewinson. 2009. ABC transporters: the power to change. *Nat. Rev. Mol. Cell Biol.* 10:218–227. doi:10.1038/nrm2646

Riordan, J.R., J.M. Rommens, B. Kerem, N. Alon, R. Rozmahel, Z. Grzelczak, J. Zielenski, S. Lok, N. Plavsic, J.L. Chou, et al. 1989. Identification of the cystic fibrosis gene: cloning and characterization of complementary DNA. *Science.* 245:1066–1073. doi:10.1126/science.2475911

Sauna, Z.E., I.W. Kim, and S.V. Ambudkar. 2007. Genomics and the mechanism of P-glycoprotein (ABCB1). *J. Bioenerg. Biomembr.* 39:481–487. doi:10.1007/s10863-007-9115-9

Schuldiner, S. 2006. Structural biology: the ins and outs of drug transport. *Nature.* 443:156–157. doi:10.1038/443156b

Sharma, S., and A.L. Davidson. 2000. Vanadate-induced trapping of nucleotides by purified maltose transport complex requires ATP hydrolysis. *J. Bacteriol.* 182:6570–6576. doi:10.1128/JB.182.23.6570-6576.2000

Smith, P.C., N. Karpowich, L. Millen, J.E. Moody, J. Rosen, P.J. Thomas, and J.F. Hunt. 2002. ATP binding to the motor domain from an ABC transporter drives formation of a nucleotide sandwich dimer. *Mol. Cell.* 10:139–149. doi:10.1016/S1097-2765(02)00576-2

Tombline, G., L.A. Bartholomew, I.L. Urbatsch, and A.E. Senior. 2004. Combined mutation of catalytic glutamate residues in the two nucleotide binding domains of P-glycoprotein generates a conformation that binds ATP and ADP tightly. *J. Biol. Chem.* 279:31212–31220. doi:10.1074/jbc.M404689200

Tsai, M.F., H. Shimizu, Y. Sohma, M. Li, and T.C. Hwang. 2009. State-dependent modulation of CFTR gating by pyrophosphate. *J. Gen. Physiol.* 133:405–419. doi:10.1085/jgp.200810186

Ueda, K., J. Komine, M. Matsuo, S. Seino, and T. Amachi. 1999. Cooperative binding of ATP and MgADP in the sulfonylurea receptor is modulated by glibenclamide. *Proc. Natl. Acad. Sci. USA.* 96:1268–1272. doi:10.1073/pnas.96.4.1268

Urbatsch, I.L., B. Sankaran, J. Weber, and A.E. Senior. 1995. P-glycoprotein is stably inhibited by vanadate-induced trapping of nucleotide at a single catalytic site. *J. Biol. Chem.* 270:19383–19390. doi:10.1074/jbc.270.33.19383

van der Does, C., and R. Tampé. 2004. How do ABC transporters drive transport? *Biol. Chem.* 385:927–933. doi:10.1515/BC.2004.121

Vergani, P., A.C. Nairn, and D.C. Gadsby. 2003. On the mechanism of MgATP-dependent gating of CFTR Cl^- channels. *J. Gen. Physiol.* 121:17–36. doi:10.1085/jgp.20028673

Vergani, P., S.W. Lockless, A.C. Nairn, and D.C. Gadsby. 2005. CFTR channel opening by ATP-driven tight dimerization of its nucleotide-binding domains. *Nature.* 433:876–880. doi:10.1038/nature03313

Ward, A., C.L. Reyes, J. Yu, C.B. Roth, and G. Chang. 2007. Flexibility in the ABC transporter MsbA: alternating access with a twist. *Proc. Natl. Acad. Sci. USA.* 104:19005–19010. doi:10.1073/pnas.0709388104

Wen, P.C., and E. Tajkhorshid. 2008. Dimer opening of the nucleotide binding domains of ABC transporters after ATP hydrolysis. *Biophys. J.* 95:5100–5110. doi:10.1529/biophysj.108.139444

Yuan, Y.R., S. Blecker, O. Martsinkevich, L. Millen, P.J. Thomas, and J.F. Hunt. 2001. The crystal structure of the MJ0796 ATP-binding cassette. Implications for the structural consequences of ATP hydrolysis in the active site of an ABC transporter. *J. Biol. Chem.* 276:32313–32321. doi:10.1074/jbc.M100758200

Zaitseva, J., S. Jenewein, T. Jumpertz, I.B. Holland, and L. Schmitt. 2005. H662 is the linchpin of ATP hydrolysis in the nucleotide-binding domain of the ABC transporter HlyB. *EMBO J.* 24:1901–1910. doi:10.1038/sj.emboj.7600657

Zeltwanger, S., F. Wang, G.T. Wang, K.D. Gillis, and T.C. Hwang. 1999. Gating of cystic fibrosis transmembrane conductance regulator chloride channels by adenosine triphosphate hydrolysis. Quantitative analysis of a cyclic gating scheme. *J. Gen. Physiol.* 113:541–554. doi:10.1085/jgp.113.4.541

Zhou, Z., X. Wang, M. Li, Y. Sohma, X. Zou, and T.C. Hwang. 2005. High affinity ATP/ADP analogues as new tools for studying CFTR gating. *J. Physiol.* 569:447–457. doi:10.1113/jphysiol.2005.095083

Zhou, Z., X. Wang, H.Y. Liu, X. Zou, M. Li, and T.C. Hwang. 2006. The two ATP binding sites of cystic fibrosis transmembrane conductance regulator (CFTR) play distinct roles in gating kinetics and energetics. *J. Gen. Physiol.* 128:413–422. doi:10.1085/jgp.200609622